Available online at www.sciencedirect.com
SCIENCE DIRECT®
ELSEVIER
Journal of Sound and Vibration 272 (2004) 169–185
JOURNAL OF SOUND AND VIBRATION
www.elsevier.com/locate/jsvi

Natural flexural vibrations of a continuous beam on discrete elastic supports ☆

R.J. Hosking[a], Saiful Azmi Husain[a,*], F. Milinazzo[b]

[a] *Department of Mathematics, Universiti Brunei Darussalam, Gadong BE1410, Brunei*
[b] *Department of Mathematics, University of Victoria, Victoria, B.C., Canada V8W 3P4*

Received 24 November 2001; accepted 20 March 2003
Dedicated to the memory of B.C. Rennie

Abstract

It has been suggested that modern rail systems might exploit so-called floating tracks, to minimise traffic vibration and noise. This paper discusses the transverse deflexion of an infinite Bernoulli–Euler beam mounted on discrete elastic supports, a model considered suitable to explore low-frequency vibrations and associated resonances in such systems. The dynamics is governed by the eigenvalues and eigenvectors of a transfer matrix, which relates the deflexion of any beam span to the deflexions of its neighbours. Important "extensive" contributions, rather than "spatially damped" modes, occur whenever the transfer matrix has one or more eigenvalues of modulus 1. Responses such as the so-called "pinned–pinned resonance" occur when these eigenvalues of modulus 1 are real (i.e., the eigenvalues are ∓ 1); and further modes corresponding to two complex conjugate eigenvalues coalescing into ∓ 1 arise at other wavelengths, when the supports are elastic—i.e., in addition to the resonant modes identified in many earlier analyses assuming fixed supports. There is no average energy flux from span to span for any mode defined by a real eigenvector, and we infer that zero-energy transfer between spans is a characteristic of the resonant response of the system to a stationary vibrating source located on some particular span.
© 2003 Elsevier Ltd. All rights reserved.

1. Introduction

Light or overhead rail ("skytrain") transport systems help to alleviate urban passenger traffic congestion, especially in very large cities such as Bangkok. It has been suggested that a composite

☆ Dedicated to the memory of B.C. Rennie, the first Professor of Mathematics at James Cook University (Australia)—who not only worked on the topic discussed here, but also lit a flickering flame of mathematical research there which a recent episode of misguided managerialism has not yet extinguished.

*Corresponding author.
E-mail address: saiful@fos.ubd.edu.bn (S.A. Husain).

0022-460X/03/$ - see front matter © 2003 Elsevier Ltd. All rights reserved.
doi:10.1016/S0022-460X(03)00325-0

rail and longitudinal concrete beam ("combined rail") mounted on discrete resilient supports, such as in a floating ladder track, may produce much less vibration and noise [1,2]. The transverse deflexion of a continuous Bernoulli–Euler beam with discrete elastic supports is discussed in this paper, as a theoretical first step to examine vibrations which may occur in a floating rail track. Our simple model may not satisfactorily predict high-frequency noise [3,4], but low-frequency vibrations and any associated resonance phenomena can be explored.

The deflexion of a continuous beam with a few rigid supports is well documented in the classical engineering literature (e.g., Ref. [5]), but the free (natural) vibration of a beam with intermediate elastic supports was not investigated until relatively recently. Kukla [6,7] obtained an nth order determinant, which defines the natural frequencies of an axially loaded beam with concentrated masses and n intermediate elastic supports. Noting the obvious disadvantage of a large order determinant when n is large, Luo [8] considered the vibration of an infinite uniform beam with equidistant discrete supports, with an axial load and viscoelastic damping included in the mathematical model. The mathematical approach adopted by Luo is favoured in this paper, but we prefer our simpler model to clarify the governing role of the eigenvalues and eigenvectors of the transfer matrix.

The mathematical model is described in Section 2, and its solution for free (natural) vibrations is discussed in Section 3, where the transfer matrix is introduced. The eigenvalues of the transfer matrix are considered in detail in Section 4, and the important distinction between "spatially damped" and "extensive" modes is made in Section 5. Energy transfer between spans is analysed in Section 6, with reference also made to an associated Appendix. Resonant extensive modes are examined in Section 7, where some specific calculations are presented. A summary of the results is given in Section 8.

2. The mathematical model

The Bernoulli–Euler equation for the small transverse deflexion $\eta(x,t)$ of a beam is

$$EI\eta_{xxxx} + m\eta_{tt} = f(x,t), \tag{1}$$

where E is the elasticity modulus and I the moment of inertia of the beam of mass m per unit length, and $f(x,t)$ is a possible forcing function due to an external load.

In this paper, the beam is assumed to be initially horizontal and infinite with equal discrete elastic supports, at points spaced a distance L apart. At every such point ($x = nL$: $n = 0, \pm 1, \pm 2, \ldots$ say), the boundary conditions to be applied to the solutions to Eq. (1) are: (i) η is continuous; (ii) $\partial\eta/\partial x$ is continuous; (iii) $\partial^2\eta/\partial x^2$ is continuous; and (iv) $\partial^3\eta/\partial x^3$ has jump discontinuity $-\gamma\eta/(EI)$, where γ is the elastic support stiffness. The effect of the elastic supports might also be represented in the governing equation, such that Eq. (1) is replaced by

$$EI\eta_{xxxx} + m\eta_{tt} + \gamma \sum_{n=-\infty}^{\infty} \delta(x - nL)\eta(x,t) = f(x,t), \tag{2}$$

where $\delta(x)$ denotes the Dirac delta function.

Although it is assumed that the beam is simply supported and always maintains its points of contact with the elastic supports, the transverse beam deflexions there (relative to the initial horizontal position) may be non-zero, since the elasticity of the supports means that these points of contact can move—unlike the more familiar case of rigid supports, where the points of contact are fixed.

3. Natural vibrations

Disturbances may persist for some time after any forcing function is removed (i.e., when $f(x,t)=0$), if the kinetic energy transfer into heat is slow. There can also be an important synergy between a forcing function and the natural vibrations of the system, such that the response of the system to particular forcing frequencies is most pronounced. This phenomenon is often explored in practice by "resonance testing", where the response of a structure to a localised stationary vibrating load is an important test of its safety. Thus free (natural) vibrations may be of interest not only mathematically but also physically, and it may be that they occur not only in the vicinity of their original source but also at significant distances away.

When $f(x,t)=0$ and the Fourier form $\eta(x,t)=\mathrm{Re}\{\eta(x)\mathrm{e}^{\mathrm{i}\omega t}\}$ is introduced into the beam equation (1), the resulting homogeneous fourth order ordinary differential equation for the spatial component of this normal mode has the well-known solution

$$\eta(x) = A_n \cosh[k(x-nL)] + B_n \sinh[k(x-nL)] + C_n \cos[k(x-nL)] + D_n \sin[k(x-nL)], \tag{3}$$

in any span $nL<x<(n+1)L$ ($n=0,\pm 1,\pm 2,\ldots$), where the inverse of the dispersion relation

$$k \equiv \left(\frac{m\omega^2}{EI}\right)^{1/4},$$

defines the non-negative wave number associated with the free undamped frequency ω. The integration constants A_n, B_n, C_n, D_n in the present context are generally complex, however (see later).

Application of the conditions stated in Section 2, at the boundaries of successive spans between the elastic supports, is algebraically simpler via the four functions

$$\frac{1}{2}\eta + \frac{1}{2k^2}\eta'' = A_n \cosh[k(x-nL)] + B_n \sinh[k(x-nL)],$$

$$\frac{1}{2}\eta - \frac{1}{2k^2}\eta'' = C_n \cos[k(x-nL)] + D_n \sin[k(x-nL)],$$

$$\frac{1}{k}\eta' = A_n \sinh[k(x-nL)] + B_n \cosh[k(x-nL)] - C_n \sin[k(x-nL)] + D_n \cos[k(x-nL)],$$

$$\frac{1}{2k^3}\eta''' - \frac{1}{2k}\eta' = C_n \sin[k(x-nL)] - D_n \cos[k(x-nL)].$$

Thus the first three of these four functions are continuous at the boundaries, and the fourth has a jump discontinuity $-\gamma\eta/(2k^3 EI)$. At the boundary $x=L$ between the two spans $0<x<L$ and

$L<x<2L$ for example, we have

$$A_0 \cosh\alpha + B_0 \sinh\alpha = A_1,$$

$$C_0 \cos\alpha + D_0 \sin\alpha = C_1,$$

$$A_0 \sinh\alpha + B_0 \cosh\alpha - C_0 \sin\alpha + D_0 \cos\alpha = B_1 + D_1,$$

$$\begin{aligned} C_0 \sin\alpha - D_0 \cos\alpha &= D_1 + 2\beta(A_1 + C_1) \\ &\equiv D_1 + 2\beta(A_0 \cosh\alpha + B_0 \sinh\alpha + C_0 \cos\alpha + D_0 \sin\alpha), \end{aligned} \tag{4}$$

where zero and unity subscripts denote the respective integration constants in each of these two adjacent spans as indicated above. The dimensionless wave number $\alpha = kL$ and the coefficient $\beta = \Gamma/\alpha^3$ introduced here, where $\Gamma = \gamma L^3/(4EI)$ defines the relative elasticity of the equidistant discrete supports, are important parameters. In this paper, special emphasis is given to the relative elasticity value $\Gamma = 25$, to calculate the response using representative physical parameters for the floating ladder track designed by Wakui et al. [2]—namely $\gamma = 1.5 \times 10^7$ N/m, $L = 1.5$ m, and $EI \approx 5 \times 10^5$ N m^2.

From Eq. (4) it follows that the respective sets of integration constants (which we shall call deflexion coefficient vectors) are related by

$$(A_1, B_1, C_1, D_1)^{\mathrm{T}} = \mathbf{M}(A_0, B_0, C_0, D_0)^{\mathrm{T}}, \tag{5}$$

in terms of the 4×4 *transfer matrix* $\mathbf{M}$ given by

$$\begin{pmatrix} \cosh\alpha & \sinh\alpha & 0 & 0 \\ \sinh\alpha - 2\beta\cosh\alpha & \cosh\alpha - 2\beta\sinh\alpha & -2\beta\cos\alpha & -2\beta\sin\alpha \\ 0 & 0 & \cos\alpha & \sin\alpha \\ 2\beta\cosh\alpha & 2\beta\sinh\alpha & 2\beta\cos\alpha - \sin\alpha & \cos\alpha + 2\beta\sin\alpha \end{pmatrix},$$

with superscript T denoting the transpose of the respective constant vectors. This relation applies for any two adjacent spans, so that beam vibrations must propagate in a fashion governed by iteration of the matrix $\mathbf{M}$ or its reciprocal $\mathbf{M}^{-1}$ (the determinant of $\mathbf{M}$ is 1): thus

$$(A_n, B_n, C_n, D_n)^{\mathrm{T}} = \mathbf{M}^n(A_0, B_0, C_0, D_0)^{\mathrm{T}}, \tag{6}$$

defines the deflexion in any nth span to the right of the span $0<x<L$ (cf. also Ref. [8]), and

$$(A_{-n}, B_{-n}, C_{-n}, D_{-n})^{\mathrm{T}} = (\mathbf{M}^{-1})^n \ (A_0, B_0, C_0, D_0)^{\mathrm{T}}, \tag{7}$$

defines the deflexion in any nth span to its left. Moreover, the vibration is governed by the eigenvalues $\{\lambda_i\colon i = 1, 2, 3, 4\}$ and the corresponding eigenvectors $\{\mathbf{v}_i\colon i = 1, 2, 3, 4\}$ of the transfer matrix $\mathbf{M}$, defined by $\mathbf{M}\mathbf{v}_i = \lambda_i \mathbf{v}_i$ $(\forall i \in \{1, 2, 3, 4\})$. As discussed in the following section, the four eigenvalues of $\mathbf{M}$ constitute two reciprocal pairs, so the eigenvalues of $\mathbf{M}^{-1}$ are identical with the eigenvalues of $\mathbf{M}$.

4. Eigenvalues of the transfer matrix

The characteristic equation for the eigenvalues of the transverse matrix $\mathbf{M}$ introduced in the previous section may be written as a quadratic

$$(\mu - \cosh\alpha + \beta\sinh\alpha)(\mu - \cos\alpha - \beta\sin\alpha) + \beta^2\sinh\alpha\sin\alpha = 0, \tag{8}$$

or

$$\begin{aligned}\mu^2 &- [\cosh\alpha + \cos\alpha - \beta(\sinh\alpha - \sin\alpha)]\mu \\ &+ \cosh\alpha\cos\alpha + \beta(\cosh\alpha\sin\alpha - \sinh\alpha\cos\alpha) = 0,\end{aligned} \tag{9}$$

where

$$2\mu \equiv \lambda + \frac{1}{\lambda}, \tag{10}$$

which is equivalent to the quartic defining the four eigenvalues $\{\lambda_i : i = 1, 2, 3, 4\}$. Thus, it is immediately apparent that the four eigenvalues constitute two reciprocal pairs, where each pair corresponds to one of the two roots of the quadratic equation in μ (cf. [3]). Also, since $\mathbf{M}\mathbf{v} = \lambda\mathbf{v}$ implies $\mathbf{M}^{-1}\mathbf{v} = \lambda^{-1}\mathbf{v}$, the matrix $\mathbf{M}$ and its reciprocal matrix $\mathbf{M}^{-1}$ have the same eigenvalues, where the eigenvector corresponding to the eigenvalue λ of $\mathbf{M}$ is the eigenvector corresponding to the eigenvalue λ^{-1} of $\mathbf{M}^{-1}$.

For "soft supports" such that $\beta \ll 1$, from Eq. (8) there are two real roots

$$\mu = \cos\alpha + \beta\sin\alpha + \beta^2\frac{\sinh\alpha\sin\alpha}{\cosh\alpha - \cos\alpha} + \mathrm{O}(\beta^4),$$

and

$$\mu = \cosh\alpha - \beta\sinh\alpha - \beta^2\frac{\sinh\alpha\sin\alpha}{\cosh\alpha - \cos\alpha} + \mathrm{O}(\beta^4),$$

yielding, respectively, $\cos\alpha$ and $\cosh\alpha$—and hence respectively eigenvalues $\lambda = \mathrm{e}^{\pm\mathrm{i}\alpha}$ of modulus 1 and real eigenvalues $\lambda = \mathrm{e}^{\pm\alpha}$—in the zero support limit $\beta \to 0$. However, the discriminant of the quadratic may be expressed as

$$\Delta = [\cosh\alpha - \cos\alpha - \beta(\sinh\alpha + \sin\alpha)]^2 - 4\beta^2\sinh\alpha\sin\alpha, \tag{11}$$

which is obviously not positive definite for all values of α and β. Thus unlike the case of a free unsupported beam corresponding to $\beta = 0$, the values of μ may be complex. Fig. 1 displays contours of the discriminant Δ in the $\alpha\beta$-plane, together with superimposed curves of the relationship $\beta = \Gamma/\alpha^3$ for various values of the parameter Γ, where some of these superimposed curves intersect both negative and positive Δ contours. For values around $\Gamma = 25$, of special interest in this paper, these curves cut through quite a large part of the $\Delta < 0$ region at smaller α (but not the small island at larger α near $\beta = 1$).

The curves for the various values of Γ in Fig. 2 show how μ depends upon α, when μ does take real values. Of major interest are regions where at least one of the two μ values has magnitude $|\mu| \leqslant 1$, such that the two corresponding eigenvalues $\lambda = \mu \pm \mathrm{i}\sqrt{1-\mu^2}$ either constitute a reciprocal complex conjugate pair each of modulus 1 (when $|\mu| < 1$) or take the real values ∓ 1 (when $|\mu| = 1$). Any eigenvalue of modulus 1 (real or imaginary) produces an "extensive" mode, in the absence of any dissipation—on the other hand, real μ with magnitude $|\mu| > 1$ such that the corresponding

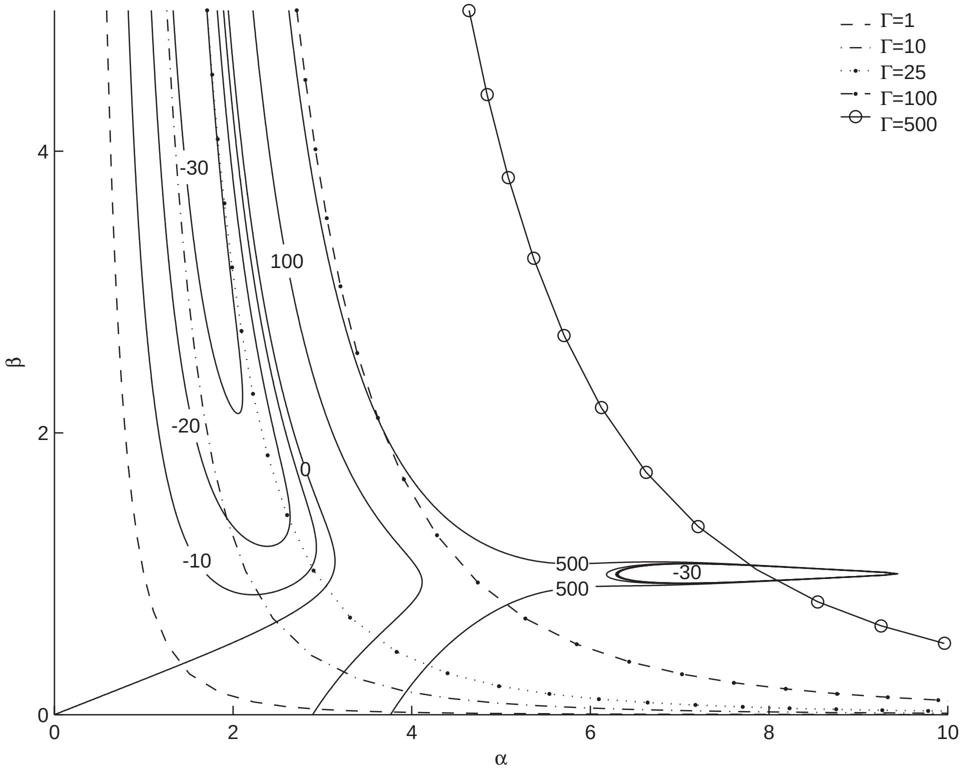

Fig. 1. Contours of discriminant Δ (solid lines for $-30, -20, -10, 0, 100, 500$) in the $\alpha\beta$-plane, with superimposed β curves for various Γ (broken lines for $1, 10, 25, 100, 500$ as indicated).

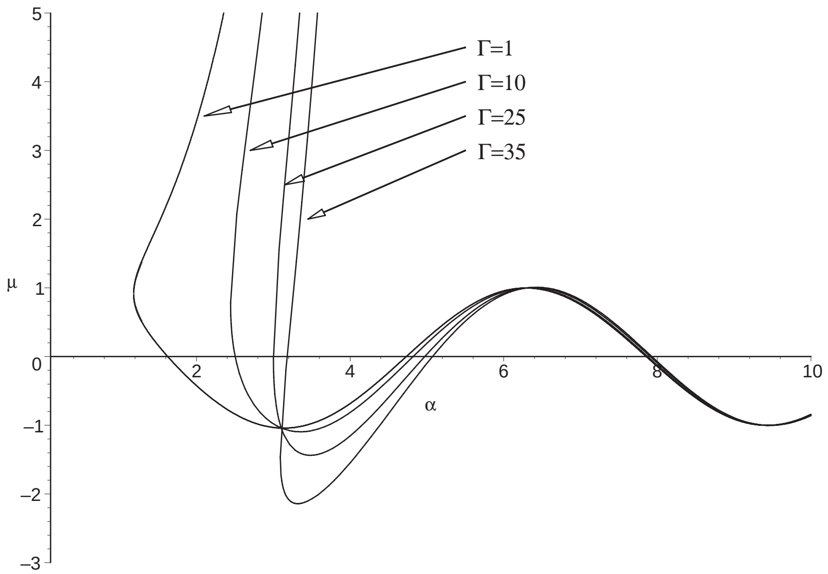

Fig. 2. Real μ curves for various $\Gamma(1, 10, 25, 35)$.

eigenvalues $\lambda = \mu \pm \sqrt{\mu^2 - 1}$ are real produces a "spatially damped" mode (see later). In passing, let us also note that by writing $\mu = \cos\theta$ such that $\lambda + 1/\lambda = 2\cos\theta$, eigenvalues of modulus 1 may be expressed in the polar form $\lambda = e^{\pm i\theta}$.

We recall that $\Gamma = 25$ is specifically representative of a floating ladder track (with physical parameters $\gamma = 1.5 \times 10^7$ N/m, $L = 1.5$ m, and EI approximately 5×10^5 N m^2). Careful computation for $\Gamma = 25$ in the real μ region showed that (cf. Fig. 2):

(1) for $3.0275 < \alpha < 3.0560$, where $0 < \mu < 1$ on the upper branch and we find $-0.5597 < \mu < 0$ on the lower branch, there are two reciprocal complex conjugate pairs of eigenvalues with modulus 1;

(2) when the upper branch of the μ curve passes through $+1$ at $\alpha \approx 3.0560$, the corresponding former complex conjugate pair coalesces into the real eigenvalue $\lambda = +1$ (repeated), while the reciprocal complex conjugate eigenvalue pair (with modulus 1) from the lower branch remains;

(3) at larger α, one of this pair of real eigenvalues corresponding to the upper branch is greater than 1 and the other is less than 1 (recall that the eigenvalues occur as reciprocal pairs)—whereas the reciprocal complex conjugate eigenvalue pair (with modulus 1) from the lower branch remains;

(4) the reciprocal pair of real eigenvalues from the upper branch *always* remains as α increases further, with the magnitude of the eigenvalue greater than 1 rapidly and monotonically increasing towards 2μ, and the magnitude of the other of course monotonically decreasing towards zero;

(5) on the other hand, when the lower branch of the μ curve passes through -1 at $\alpha = \pi$, the reciprocal complex conjugate pair of eigenvalues (with modulus 1) associated with the lower branch coalesces into the real eigenvalue -1 (repeated);

(6) then for $\alpha > \pi$ there is an interval with $\mu < -1$, where this pair of eigenvalues corresponding to the lower branch of the μ curve are also real, with one of magnitude greater than 1 and the other of course of magnitude less than 1 (i.e., the former reciprocal complex conjugate pair of eigenvalues are replaced by another reciprocal pair of real eigenvalues);

(7) when the lower branch of the μ curve again passes through -1 (in this case at $\alpha \approx 4.1315$), this second pair of real eigenvalues coalesces into $\lambda = -1$ (repeated);

(8) for even larger α where $|\mu| < 1$, the second pair of real eigenvalues associated with the lower branch of the μ curve is again replaced by a reciprocal complex conjugate pair of eigenvalues (with modulus 1)—until this branch passes through 1 at $\alpha = 2\pi$, when this pair coalesces into the real eigenvalue $\lambda = +1$ (repeated);

(9) then for $\alpha > 2\pi$ there is a narrow interval with $\mu > 1$, where the pair of eigenvalues corresponding to the lower branch of the μ curve are again real, with one of magnitude greater than 1 and the other of magnitude less than 1; and so on.

The complex conjugate pair of μ values represented in Fig. 3 correspond to the intersection of the $\Gamma = 25$ curve with the negative discriminant (negative Δ) region at smaller non-zero values of α in Fig. 1, as is also typical for other Γ values shown in Fig. 2. Relation (10) then yields four complex eigenvalues, constituting two complex conjugate pairs, where each member of one pair is the reciprocal of a member of the other pair. However, for $\Gamma = 25$ the range of α where there are such eigenvalues of modulus 1 is very narrow (just to the left of $\alpha = 3.0275$).

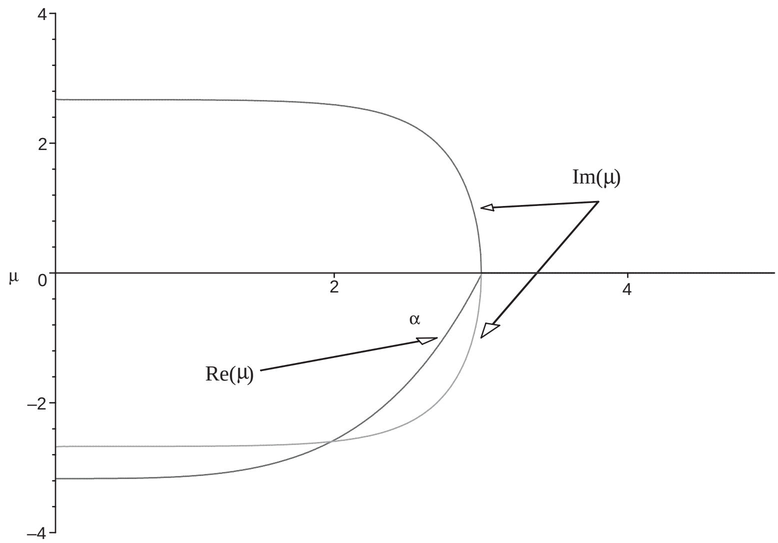

Fig. 3. Complex μ curve for $\Gamma = 25$ (real and imaginary parts of the complex conjugate pair).

Important features of the behaviour can be defined analytically. Thus from (9), modes corresponding to the eigenvalue $\lambda = -1$ (when $\mu = -1$) occur where

$$\left[\cosh\frac{\alpha}{2}\cos\frac{\alpha}{2}\right]^2\left[1-\beta\left(\tanh\frac{\alpha}{2}-\tan\frac{\alpha}{2}\right)\right] = 0, \tag{12}$$

and those corresponding to $\lambda = +1$ (when $\mu = +1$) occur where

$$\left[\sinh\frac{\alpha}{2}\sin\frac{\alpha}{2}\right]^2\left[1-\beta\left(\coth\frac{\alpha}{2}+\cot\frac{\alpha}{2}\right)\right] = 0. \tag{13}$$

Thus $\lambda = -1$ at $\alpha = (2m+1)\pi$ where $m = 0, \pm 1, \pm 2, \ldots$, and for $\beta \neq 0$ also at values of α given by

$$1-\beta\left(\tanh\frac{\alpha}{2}-\tan\frac{\alpha}{2}\right) = 0, \tag{14}$$

and $\lambda = +1$ at $\alpha = 2m\pi$ where $m = 0, \pm 1, \pm 2, \ldots$, and for $\beta \neq 0$ also at values of α given by

$$1-\beta\left(\coth\frac{\alpha}{2}+\cot\frac{\alpha}{2}\right) = 0. \tag{15}$$

One may deduce that there are always ranges of α near $\alpha = m\pi$ ($m = \pm 1, \pm 2, \ldots$) where $|\mu| > 1$, although these ranges narrow as the wave number increases (cf. again Fig. 2). Thus for $\alpha \gg 1$ (when $\beta = \Gamma/\alpha^3 \ll 1$) the transcendental equations (14) and (15) reduce to $\cot(\alpha/2) \approx -\beta$ and $\tan(\alpha/2) \approx \beta$, respectively, hence $\mu < -1$ on intervals where $\alpha > (2m+1)\pi$ (for $m = 0, 1, 2, \ldots$) and $\mu > 1$ on intervals where $\alpha > 2m\pi$ (for $m = 1, 2, \ldots$). These results also follow directly from Eq. (9) for $\beta \ll 1$, previously associated with "soft supports", but where $\mu = \cos\alpha + \beta\sin\alpha + O(\beta^2)$ now defines the smaller root and the second root has the exponentially large value $\mu = \cosh\alpha - \beta\sinh\alpha + O(\beta^2)$, for sufficiently large α.

5. Spatially damped and extensive modes

Let us first consider the simplest case, where the deflexion coefficient vector in the span $0<x<L$ is proportional to the eigenvector $\mathbf{v}$ corresponding to an eigenvalue λ of the transfer matrix $\mathbf{M}$. Thus for $(A_0, B_0, C_0, D_0)^{\mathrm{T}} = c\mathbf{v}$ where c is a constant, from Eq. (6) the deflexion coefficient vector in any nth span to the right ($nL<x<(n+1)L$) is then

$$(A_n, B_n, C_n, D_n)^{\mathrm{T}} = \lambda^n (A_0, B_0, C_0, D_0)^{\mathrm{T}},$$

and from Eq. (7) the deflexion coefficient vector in any nth span to the left ($-(n+1)L<x<-nL$) is

$$(A_{-n}, B_{-n}, C_{-n}, D_{-n})^{\mathrm{T}} = \left(\frac{1}{\lambda}\right)^n (A_0, B_0, C_0, D_0)^{\mathrm{T}}.$$

Moreover, Eq. (3) for the beam deflexion in any nth span to the right, therefore may be expressed as $\eta(x) = (A_n, B_n, C_n, D_n)\mathbf{w}_n = c\lambda^n \mathbf{v}^{\mathrm{T}}\mathbf{w}_n$ where

$$\mathbf{w}_n^{\mathrm{T}} = (\cosh[k(x-nL)], \sinh[k(x-nL)], \cos[k(x-nL)], \sin[k(x-nL)]), \tag{16}$$

or analogously involving the reciprocal eigenvalue for the deflexion in any nth span to the left.

More generally, for all values of α such that the four eigenvalues $\{\lambda_i : i = 1, 2, 3, 4\}$ of the transfer matrix $\mathbf{M}$ are distinct, the four corresponding eigenvectors $\{\mathbf{v}_i : i = 1, 2, 3, 4\}$ are linearly independent (cf. Ref. [9], for example). Then any deflexion coefficient vector in the span $0<x<L$ may be expressed as a linear combination of the four eigenvectors—namely

$$(A_0, B_0, C_0, D_0)^{\mathrm{T}} = c_1\mathbf{v}_1 + c_2\mathbf{v}_2 + c_3\mathbf{v}_3 + c_4\mathbf{v}_4, \tag{17}$$

where the c_i are constants. Thus from Eq. (6) the deflexion coefficient vector in any nth span to the right is

$$(A_n, B_n, C_n, D_n)^{\mathrm{T}} = \lambda_1^n c_1\mathbf{v}_1 + \lambda_2^n c_2\mathbf{v}_2 + \lambda_3^n c_3\mathbf{v}_3 + \lambda_4^n c_4\mathbf{v}_4, \tag{18}$$

and the deflexion $\forall n \in \{0, 1, 2, 3, \ldots\}$ is

$$\eta(x) = c_1\lambda_1^n\mathbf{v}_1^{\mathrm{T}}\mathbf{w}_n + c_2\lambda_2^n\mathbf{v}_2^{\mathrm{T}}\mathbf{w}_n + c_3\lambda_3^n\mathbf{v}_3^{\mathrm{T}}\mathbf{w}_n + c_4\lambda_4^n\mathbf{v}_4^{\mathrm{T}}\mathbf{w}_n \tag{19}$$

with $\mathbf{w}_n$ again the basis vector as defined above. In analogous expressions for spans to the left, each of the eigenvalues is of course replaced by its reciprocal.

However, to ensure that the deflexions (either to the right or the left) remain bounded as $n \to \infty$, only those terms involving real or complex eigenvalues with modulus less than or equal to 1 (i.e., $|\lambda| \leqslant 1$) may be retained. Thus any term in Eq. (17) or (19) involving an eigenvalue with modulus greater than 1 must be removed, by setting its coefficient zero (cf. also Ref. [8]), whereas this term remains in the analogous expressions for spans to the left (since the eigenvalue involved is the respective reciprocal). On the other hand, any term in Eq. (17) or (19) involving an eigenvalue with modulus less than 1—or in analogous expressions for spans to the left, a reciprocal eigenvalue of modulus less than 1—vanishes as $n \to \infty$, so such terms are "spatially damped". In contrast, any term involving a real or complex eigenvalue of modulus 1 persists as $n \to \infty$, and is a part of the ultimately dominant "extensive" deflexion—i.e., the deflexion component which is not spatially damped. Let us now recall the hierarchical behaviour of the eigenvalues, as described in the preceding section.

At any α where μ is real and there is a branch on which $|\mu| > 1$, there is a reciprocal pair of real eigenvalues, one of which is greater than 1 and the other less than 1. For deflexions to the right, the first of these real eigenvalues is rejected and the second produces a spatially damped component; for deflexions to the left, which is of course governed by eigenvalue reciprocals, the first produces a spatially damped component and the second is rejected. Thus the corresponding deflexion components split into distinctive spatially damped forms, to the right and to the left. At those α values where μ is real and $|\mu| > 1$ on both branches, such that all four eigenvalues are real, this is true for the total deflexion. The case of complex μ at smaller α values is similar, since two of the four resulting complex eigenvalues have modulus greater than 1 and the other two (their reciprocals) have modulus less than 1.

However, there is always at least one reciprocal pair of complex conjugate eigenvalues of modulus 1 for real μ at any α where $|\mu| < 1$, which is therefore a sufficient condition for an extensive deflexion component. Let us recall that for values of α where $|\mu| = 1$, a former reciprocal pair of complex conjugate eigenvalues coalesces into $\lambda = -1$ (repeated) when $\mu = -1$ or $\lambda = +1$ (repeated) when $\mu = +1$, respectively. As discussed later, in these cases resonant extensive modes characterised by zero average energy transfer occur, although the deflexion in one span (say $0 < x < L$) may be successively "twinned" in every other span. The transfer matrix $\mathbf{M}$ is degenerate when one of the eigenvalues is repeated, such that with $\lambda = \mp 1$ of algebraic multiplicity 2 there is geometric multiplicity 1 (i.e., only one corresponding eigenvector), although other linearly independent basis vectors are usually constructed in order to span the vector space. Hence when $\lambda_4 = \lambda_1$ (say) in our context, the form of the general solution replacing Eq. (19) is

$$\eta(x) = (c_1\lambda_1^n + nc_4)\mathbf{v}_1^{\mathrm{T}}\mathbf{w}_n + c_2\lambda_2^n\mathbf{v}_2^{\mathrm{T}}\mathbf{w}_n + c_3\lambda_3^n\mathbf{v}_3^{\mathrm{T}}\mathbf{w}_n + c_4\lambda_1^n\mathbf{v}_4^{\mathrm{T}}\mathbf{w}_n, \tag{20}$$

with $\mathbf{v}_4$ constructed such that $(\mathbf{M} - \lambda_1\mathbf{I})\mathbf{v}_4 = \mathbf{v}_1$ where $\mathbf{I}$ is the unit matrix. However, the constant c_4 must be set to zero in this expression, to again ensure that the deflexions remain bounded as $n \to \infty$. Thus in effect a reduced form of Eq. (19), without the fourth term on the right-hand side, remains applicable—and in addition of course, any term involving an eigenvalue of modulus greater than 1 is also omitted, as discussed above.

6. Energy transfer

Multiplying the Bernoulli–Euler equation (1) by the time derivative of the complex conjugate $\eta^*(x,t)$ of the deflexion, followed by an integration over the nth span $nL < x < (n+1)L$, yields the time rate of change of its total (kinetic and potential) energy:

$$\frac{\mathrm{d}}{\mathrm{d}t}\int_{nL}^{(n+1)L}\left(\frac{1}{2}m\left|\frac{\partial\eta}{\partial t}\right|^2 + \frac{1}{2}EI\left|\frac{\partial^2\eta}{\partial x^2}\right|^2\right)\mathrm{d}x = \mathrm{Re}\left[EI\left(-\frac{\partial\eta^*}{\partial t}\frac{\partial^3\eta}{\partial x^3} + \frac{\partial^2\eta^*}{\partial x\partial t}\frac{\partial^2\eta}{\partial x^2}\right)\right]_{nL}^{(n+1)L}. \tag{21}$$

The terms on the right side of Eq. (21) represent the energy flux through the span, and their time average over any oscillation suitably defines the energy transfer. The first involves the shear $-EI\partial^3\eta/\partial x^3$ and the second term the bending moment $EI\partial^2\eta/\partial x^2$, in relevant products with the complex conjugates of the beam velocity and angular velocity for the shear and bending energy rates, respectively.

Let us now proceed to consider the time-averaged contributions to the energy flux in detail, from the various normal modes defined by the solution form established in Section 3. Thus the *real* basis set for the deflexion $\eta(x,t) = \mathrm{Re}\{\eta(x)\mathrm{e}^{\mathrm{i}\omega t}\}$ over the nth span consists of eight terms—namely

$$\begin{aligned}&\{\cosh[k(x-nL)]\cos(\omega t),\ \cosh[k(x-nL)]\sin(\omega t),\\&\ \sinh[k(x-nL)]\cos(\omega t),\ \sinh[k(x-nL)]\sin(\omega t),\\&\ \cos[k(x-nL)]\cos(\omega t),\ \cos[k(x-nL)]\sin(\omega t),\\&\ \sin[k(x-nL)]\cos(\omega t),\ \sin[k(x-nL)]\sin(\omega t)\}.\end{aligned}$$

The average of each of the consequent products for the two quadratic forms on the right side of Eq. (21) may be represented by 8×8 matrix displays, where rows and columns correspond to the eight real basis functions and indicate their input into the left and right components of the two quadratic forms, respectively (cf. the Appendix). Hence in combination we have the remarkably simple analogous matrix display for the average energy flux per oscillation:

$$\begin{pmatrix} 0 & 0 & 0 & 1 & 0 & 0 & 0 & 0\\ 0 & 0 & -1 & 0 & 0 & 0 & 0 & 0\\ 0 & -1 & 0 & 0 & 0 & 0 & 0 & 0\\ 1 & 0 & 0 & 0 & 0 & 0 & 0 & 0\\ 0 & 0 & 0 & 0 & 0 & 0 & 0 & -1\\ 0 & 0 & 0 & 0 & 0 & 0 & 1 & 0\\ 0 & 0 & 0 & 0 & 0 & 1 & 0 & 0\\ 0 & 0 & 0 & 0 & -1 & 0 & 0 & 0 \end{pmatrix}.$$

Consequently, the real quadratic form

$$\mathrm{i}EI\omega k^3(A_nB_n^* - A_n^*B_n + C_n^*D_n - C_nD_n^*) = EI\omega k^3\mathbf{a}_n^{\dagger}\mathbf{N}\mathbf{a}_n, \tag{22}$$

defines the average energy flux from left to right through the nth span, where the deflexion coefficient vector $(A_n, B_n, C_n, D_n)^{\mathrm{T}}$ in the nth span is now conveniently denoted by $\mathbf{a}_n$, the matrix

$$\mathbf{N} = \begin{pmatrix} 0 & -\mathrm{i} & 0 & 0\\ \mathrm{i} & 0 & 0 & 0\\ 0 & 0 & 0 & \mathrm{i}\\ 0 & 0 & -\mathrm{i} & 0 \end{pmatrix},$$

and the dagger denotes the complex conjugate transpose. In the next span to the right—i.e., in $(n+1)L < x < (n+2)L$, where the transfer matrix produces the deflexion coefficient vector $\mathbf{M}\mathbf{a}_n$—result (22) remains. This follows because the matrix quadratic form $\mathbf{a}_n^{\dagger}\mathbf{M}^{\mathrm{T}}\mathbf{N}\mathbf{M}\mathbf{a}_n \equiv \mathbf{a}_n^{\dagger}\mathbf{N}\mathbf{a}_n$ since $\mathbf{M}^{\mathrm{T}}\mathbf{N}\mathbf{M} = \mathbf{N}$, as may be shown directly. Result (22) also applies in the immediate span to the left—i.e., in $(n-1)L<x<nL$, where the deflexion coefficient vector is $\mathbf{M}^{-1}\mathbf{a}_n$—because $\mathbf{N}^{-1}\equiv\mathbf{N}$ and $\mathbf{a}_n^{\dagger}(\mathbf{M}^{-1})^{\mathrm{T}}\mathbf{N}^{-1}\mathbf{M}^{-1}\mathbf{a}_n\equiv\mathbf{a}_n^{\dagger}\mathbf{N}\mathbf{a}_n$. Thus the energy flux from some distant source to the left is identical through any span; and the same may be said for a distant source to the right, when the energy propagates in the opposite direction (right to left).

7. Resonance

Although an extensive deflexion occurs whenever there is a real or complex eigenvalue of modulus 1, the real eigenvalues $\lambda=\mp1$ at certain values of α are particularly important. Indeed, it now emerges that zero-energy transfer from span to span characterises the resonant response of the beam to a stationary vibrating load.

Let us first recall from Section 4 that the reciprocal pair of complex conjugate eigenvalues (of modulus 1) for $\alpha<\pi$, arising when the lower branch of the real μ curve for $\Gamma=25$ in Fig. 2 first passes through -1, coalesces into the repeated eigenvalue $\lambda=-1$ at $\alpha=\pi$—i.e., when $k=\pi/L$. From the discussion in Section 5, the extensive mode at $\alpha=\pi$ is given by the simple form (where c is a constant)

$$\eta(x)=(-1)^n c\sin\left[\pi\left(\frac{x}{L}-n\right)\right]\quad(n=0,\pm1,\pm2,\ldots),\tag{23}$$

since the corresponding eigenvector is $\mathbf{v}=(0,0,0,1)$ and the other two eigenvalues are real but not of magnitude 1. Eq. (23) defines the fundamental mode sometimes referred to as the "first pinned–pinned resonance" (cf. Fig. 4(a) for $c=1$ and $L=1.5$ m). It is notable that Eq. (22) implies there is no average energy flux from span to span. Similarly, at $\alpha=2\pi$ the real eigenvalue $\lambda=+1$ of multiplicity 2 with eigenvector $\mathbf{v}=(0,0,0,1)$ produces the mode (cf. Fig. 4(b) for $c=1$ and $L=1.5$ m)

$$\eta(x)=c\sin\left[2\pi\left(\frac{x}{L}-n\right)\right]\quad(n=0,\pm1,\pm2,\ldots).\tag{24}$$

From Eq. (12) we know that $\lambda=-1$ also occurs at $\alpha=(2m+1)\pi$, where $m=1,2,\ldots$, and from Eq. (13) that $\lambda=+1$ also occurs at $\alpha=2m\pi$ where $m=2,3,\ldots$. Thus there are two countably infinite sets of resonant extensive modes with elements of sine form analogous to Eq. (23) or (24) and progressively higher wave numbers (shorter wavelengths), producing no average energy flux from span to span. For these resonant "pinned–pinned" modes, it is notable that the deflexion is zero at the supports.

However, let us now recall from Section 4 that when $\beta\neq0$ there are also other values of α where $|\mu|=1$ such that $\lambda=-1$ or $+1$, given by Eqs. (14) and (15), respectively. From the lower branch of the real μ curve for $\Gamma=25$ shown in Fig. 2, for each of the above values of α there is another somewhat larger value at which the reciprocal complex conjugate pair again coalesces into the same repeated eigenvalue (alternately $\lambda=-1$ and $+1$) of multiplicity 2 and the other two eigenvalues are real but not of magnitude 1, commencing with $\lambda=-1$ at $\alpha\approx4.1315>\pi$ and $\lambda=+1$ at $\alpha\approx6.4845>2\pi$. The corresponding extensive modes are discussed below and are found to be non-zero at the discrete supports, which are not fixed but elastic and therefore may move vertically, as mentioned in Section 2.

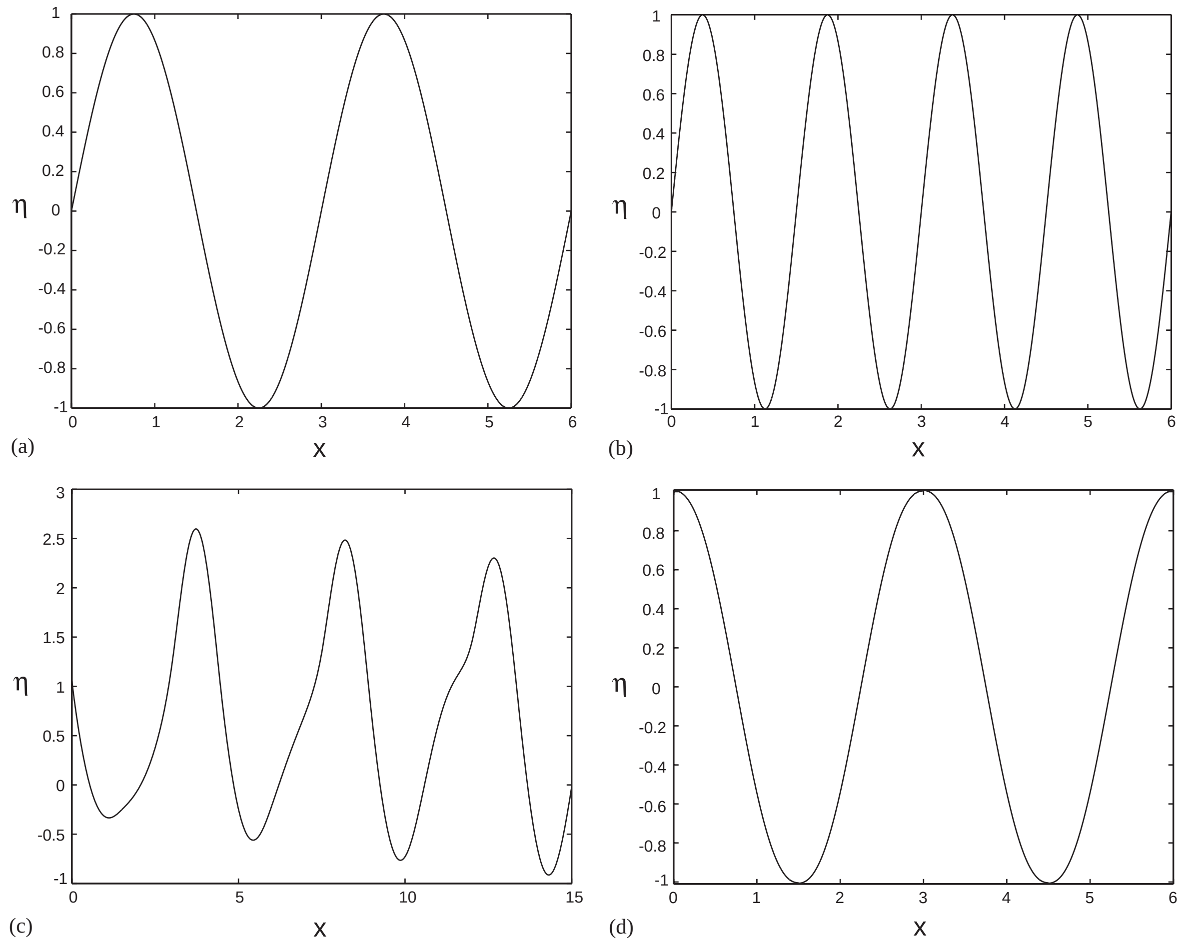

Fig. 4. (a) First pinned–pinned resonance (extensive mode at $\alpha = \pi$). (b) Second pinned–pinned resonance (extensive mode at $\alpha = 2\pi$). (c) Elastic support deflexion profile (an extensive form at $\alpha = 3.05600517$). (d) Elastic support resonance (extensive mode at $\alpha = 4.1315$).

In contrast, on the upper branch of the real μ curve there is only one non-zero value ($\alpha \approx 3.0560 < \pi$ for $\Gamma = 25$) where $|\mu| = 1$. Here one of two reciprocal complex conjugate pairs of eigenvalues of modulus 1 coalesces into $\lambda = +1$ (repeated) given by Eq. (15), but the other complex conjugate pair remains. It proved necessary to evaluate this α value very accurately (as $\alpha = 3.05600517$), to ensure that the eigenvalues (all of modulus 1) were accurately rendered as $\{+1, +1, -0.5597 \pm 0.8287i\}$, and the relevant eigenvectors as $(0.6134, -0.5582, 0.0239, 0.5582)$ and the complex pair $(0.1731 \pm 0.3268i, -0.2086 \mp 0.3320i, 0.0358 \pm 0.0676i, -0.4727 \pm 0.6928i)$. The component of the extensive deflexion defined by the real eigenvector corresponding to $\lambda = +1$ (repeated) is smoothly periodic, but this is obscured by the two other contributions from the complex conjugate eigenvalues and eigenvectors, unless of course the real eigenvector alone defines the deflexion in some span. Moreover, there may be zero average energy flux from span to span when all of these three contributions are included, such as with $c_i = 1$ for $i = 1, 2, 3$ but

$c_4 = 0$ (to omit the increasing component due to the degeneracy) in representation (20) for the deflexion, as shown in Fig. 4(c) for $L = 1.5$ m. Thus at $\alpha \approx 3.0560$ the form of the extensive deflexion predicted is *not* unique within an arbitrary scale factor c, unlike the familiar "pinned–pinned" resonances discussed above.

For values of α where $|\mu| = 1$ on the lower branch of the μ curve, but which are not multiples of π, the repeated eigenvalues $\lambda = -1$ and $+1$ (of multiplicity 2) and corresponding real eigenvectors again determine unique extensive modes at those wave numbers (within an arbitrary scale factor). Thus when $\Gamma = 25$ and $\alpha \approx 4.1315$, the repeated eigenvalue $\lambda = -1$ and the eigenvector $(0.3840, -0.3965, 0.7345, 0.3947)$ yield the extensive mode

$$\eta(x) = c(-1)^n\Big\{0.3840\cosh\Big[4.1315\Big(\frac{x}{L}-n\Big)\Big] - 0.3965\sinh\Big[4.1315\Big(\frac{x}{L}-n\Big)\Big] + 0.7345\cos\Big[4.1315\Big(\frac{x}{L}-n\Big)\Big] + 0.3947\sin\Big[4.1315\Big(\frac{x}{L}-n\Big)\Big]\Big\}, \tag{25}$$

for $n = 0, \pm1, \pm2, \ldots$—cf. Fig. 4(d), where again $L = 1.5$ m but in this case the scale factor has been chosen to be $c = 0.9$, to render a mode of unit magnitude. However, unlike the "pinned–pinned" resonances, it is notable that the amplitude maxima occur at the elastic supports. When $\alpha \approx 6.4845$, the repeated eigenvalue $\lambda = +1$ and corresponding eigenvector $(0.0998, -0.0995, 0.9850, 0.0992)$ yield the extensive mode

$$\eta(x) = c\,\Big\{0.0998\cosh\Big[6.4845\Big(\frac{x}{L}-n\Big)\Big] - 0.0995\sinh\Big[6.4845\Big(\frac{x}{L}-n\Big)\Big] + 0.9850\cos\Big[6.4845\Big(\frac{x}{L}-n\Big)\Big] + 0.0992\sin\Big[6.4845\Big(\frac{x}{L}-n\Big)\Big]\Big\}, \tag{26}$$

for $n = 0, \pm1, \pm2, \ldots$, with a wavelength half that of the $\alpha = 4.1315$ mode and with amplitude maxima again occurring at the elastic supports. There is of course no average energy transfer from span to span in either case, since each respective eigenvector is real. Thus two resonant "elastic support" extensive modes have been identified, with respective deflexions given by Eqs. (25) and (26) distinguished by maxima at the supports, but apart from a phase shift are otherwise in one-to-one correspondence with the $\alpha = \pi$ and 2π "pinned–pinned" resonances with respective deflexions given by Eqs. (23) and (24). Larger wave number (shorter wavelength) "elastic support" modes, at the successively larger values of α where $|\mu| = 1$ but which are not multiples of π, may likewise be identified.

In passing, one may of course also determine the form of any spatially damped mode (corresponding to an acceptable eigenvalue, or acceptable reciprocal eigenvalue, of modulus less than 1). In Section 4, we observed that the reciprocal pair of eigenvalues corresponding to the upper branch of the real μ curve are real after this branch passes through $+1$ (i.e., for any α greater than about 3.0560), and one of the pair has magnitude less than 1. A spatially damped mode is defined by this eigenvalue of magnitude less than 1, not only for spans to the right but also for spans to the left, since it is equivalent to the reciprocal of the eigenvalue of magnitude greater than 1. Thus with wave numbers of the resonant extensive modes particularly in mind, at $\alpha = \pi$ the relevant acceptable eigenvalue (or reciprocal eigenvalue) of magnitude less than 1 was calculated to be 0.2310, with the corresponding real eigenvector $\{0.7129, -0.7013, 0, 0.2157\}$; and at $\alpha \approx 4.1315$ it was found to be 0.0247, with the corresponding real eigenvector $\{-0.7072, 0.7070, 0.0099, 0.0068\}$. The amplitudes of the associated spatially damped modes therefore involve factors $0.2310^{|n|}$ and $0.0247^{|n|}$, respectively, for $n = 0, \pm 1, \pm 2, \ldots$; and consequently, the amplitude of the spatially damped mode at $\alpha = \pi$ or $\alpha \approx 4.1315$ becomes negligible beyond one or two adjacent spans in each direction, even if it is comparable with the amplitude of the extensive mode at some span. Amplitudes of the spatially damped modes at larger resonant wave numbers attenuate even more, since the relevant real eigenvalue rapidly tends to zero as α increases.

The frequencies in cycles per second for any mode may be calculated from the dispersion relation

$$f \equiv \frac{\omega}{2\pi} = \sqrt{\frac{EI\alpha^4}{4\pi^2 m L^4}}.$$

Physical parameters for the floating ladder track ($EI \approx 5 \times 10^5$ N m^2, $m = 300$ kg/m, $L = 1.5$ m) give approximately $f = 29$ at $\alpha = \pi$ and $f = 114$ at $\alpha = 2\pi$; and $f = 27$ at $\alpha \approx 3.0560$ and $f = 49$ at $\alpha \approx 4.1315$.

8. Summary

The natural vibration of a continuous beam on equidistant discrete elastic supports is defined by the eigenvalues and eigenvectors of a transfer matrix, which relates the deflexion coefficient vector for any one span to the deflexion coefficient vector at any other. At any wave number, the four real or complex eigenvalues of the transfer matrix occur in reciprocal pairs. Any eigenvalue with modulus less than or equal to 1 is acceptable, but only eigenvalues of modulus precisely 1 yield extensive modes, characterised by non-zero amplitudes on every span (in the absence of dissipation). Eigenvalues of modulus less than 1 yield spatially damped modes—i.e., deflexion contributions with amplitudes vanishing at a distance from a particular displaced span. An energy integral formulation of the mathematical problem provides further insight. Important resonant extensive modes correspond to repeated eigenvalues ∓ 1 and zero average energy flux between spans.

Acknowledgements

It is a pleasure to acknowledge several discussions with Hajime Wakui and his engineering colleagues in the Railway Dynamics Division at the Railway Technical Research Institute of Japan Railways, Tokyo. One of us (RJH) is also very grateful for the generous financial support of the Japan Society for the Promotion of Science, and ancillary support from the Australian Academy of Science. This paper was completed under a more recent Research Grant from Universiti Brunei Darussalam, which fostered our trans-Pacific collaboration.

Appendix

The time average of

$$2\left(\frac{\partial \eta_i}{\partial t}\frac{\partial^3 \eta_j}{\partial x^3} + \frac{\partial \eta_j}{\partial t}\frac{\partial^3 \eta_i}{\partial x^3}\right),$$

is represented by the matrix display

$$\begin{pmatrix} 0 & 0 & 0 & -1 & 0 & -p & 0 & r \\ 0 & 0 & 1 & 0 & p & 0 & -r & 0 \\ 0 & 1 & 0 & 0 & 0 & q & 0 & s \\ -1 & 0 & 0 & 0 & -q & 0 & -s & 0 \\ 0 & p & 0 & -q & 0 & 0 & 0 & 1 \\ -p & 0 & q & 0 & 0 & 0 & -1 & 0 \\ 0 & -r & 0 & -s & 0 & -1 & 0 & 0 \\ r & 0 & s & 0 & 1 & 0 & 0 & 0 \end{pmatrix},$$

where

$$p \equiv \cosh[k(x-nL)]\sin[k(x-nL)] - \sinh[k(x-nL)]\cos[k(x-nL)],$$
$$q \equiv \cosh[k(x-nL)]\cos[k(x-nL)] - \sinh[k(x-nL)]\sin[k(x-nL)],$$
$$r \equiv \cosh[k(x-nL)]\cos[k(x-nL)] + \sinh[k(x-nL)]\sin[k(x-nL)],$$

and

$$s \equiv \sinh[k(x-nL)]\cos[k(x-nL)] + \cosh[k(x-nL)]\sin[k(x-nL)].$$

Similarly, the time average of

$$2\left(\frac{\partial^2\eta_i}{\partial x\partial t}\frac{\partial^2\eta_j}{\partial x^2} + \frac{\partial^2\eta_j}{\partial x\partial t}\frac{\partial^2\eta_i}{\partial x^2}\right)$$

is

$$\begin{pmatrix} 0 & 0 & 0 & 1 & 0 & -p & 0 & r \\ 0 & 0 & -1 & 0 & p & 0 & -r & 0 \\ 0 & -1 & 0 & 0 & 0 & q & 0 & s \\ 1 & 0 & 0 & 0 & -q & 0 & -s & 0 \\ 0 & p & 0 & -q & 0 & 0 & 0 & -1 \\ -p & 0 & q & 0 & 0 & 0 & 1 & 0 \\ 0 & -r & 0 & -s & 0 & 1 & 0 & 0 \\ r & 0 & s & 0 & -1 & 0 & 0 & 0 \end{pmatrix}.$$

Half the difference of these two matrix displays yields the matrix display in Section 6, representing the time average of the energy flux defined by Eq. (21).

References

[1] H. Wakui, Ladder sleepers perform well in tests, *Railway Gazette International* 159 (1997) 589–592.

[2] H. Wakui, N. Matsumoto, H. Inoue, Technological innovation in railway structure system with ladder track system, *Proceedings of the World Congress on Railway Research* (*WCRR '97*), Vol. B, Florence, 1997 pp. 61–67.

[3] S.L. Grassie, R.W. Gregory, D. Harrison, K.L. Johnson, The dynamic response of railway track to high frequency vertical excitation, *Journal of Mechanical Engineering Science* 24 (1982) 77–90.
[4] T.X. Wu, D.J. Thompson, A double Timoshenko beam model for vertical vibration analysis of railway track at high frequencies, *Journal of Sound and Vibration* 224 (1999) 329–348.
[5] C.M. Harris, C.E. Crede, *Shock and Vibration Handbook*, Vol. 1, McGraw-Hill, New York, 1961, pp. 7–19 to 7–22.
[6] S. Kukla, The Green function method in frequency analysis of a beam with intermediate elastic supports, *Journal of Sound and Vibration* 149 (1991) 154–159.
[7] S. Kukla, Free vibrations of axially loaded beams with concentrated masses and intermediate elastic supports, *Journal of Sound and Vibration* 172 (1994) 449–458.
[8] Y. Luo, Frequency analysis of infinite continuous beam under axial loads, *Journal of Sound and Vibration* 213 (1998) 791–800.
[9] J.H. Wilkinson, *The Algebraic Eigenvalue Problem*, Oxford University Press, Oxford, 1965, pp. 4–5.